

Rational Design of Heterodimeric Protein Using Domain Swapping for Myoglobin**

Ying-Wu Lin, Satoshi Nagao, Mohan Zhang, Yasuhito Shomura, Yoshiki Higuchi, and Shun Hirota*

Abstract: Protein design is a useful method to create novel artificial proteins. We developed a rational approach to design a heterodimeric protein using domain swapping for horse myoglobin (Mb). As confirmed by X-ray crystallographic analysis, a heterodimeric Mb with two different active sites was produced efficiently from two surface mutants of Mb, in which the charges of two amino acids involved in the dimer salt bridges were reversed in each mutant individually, with the active site of one mutant modified. This study shows that the method of constructing heterodimeric Mb with domain swapping is useful for designing artificial multi-heme proteins.

Protein design is a powerful tool for creating novel artificial proteins by redesigning natural proteins or designing *de novo* proteins.^[1] Successful examples include artificial oxidases,^[2] reductases,^[3] and hydrolases.^[4] To produce an artificial protein, it is crucial to control its folding, which may be achieved by controlling the interaction between secondary structures using metal ions or cofactors.^[5] Protein dimerization may also be used to control the folding and biological functions. For example, human soluble guanylate cyclase for NO-signal transduction is a heterodimer consisting of α and β subunits (α and $\beta\beta$ homodimers also exist).^[6] Recently, Roelfes and co-workers designed an artificial metalloenzyme catalyzing the Diels-Alder reaction based on a dimeric transcription factor (lactococcal multidrug resistance regulator).^[7] Development of other methods to design dimeric or oligomeric proteins is indispensable to broaden the variety of artificial enzymes.

Domain swapping is a phenomenon in which a helix or a secondary structure is exchanged between protein molecules. It has been observed in many proteins and associated with protein folding and function.^[8] These proteins include prion,^[9] cystatin C,^[10] β -microglobulin,^[11] and serpin,^[12] which are involved in deposition diseases. Domain swapping has also been observed for heme proteins,^[13] including cytochrome *c* (cyt *c*)^[14] and myoglobin (Mb)^[15]. Recently, we found that intermolecular hydrophobic interaction in cyt *c*

at the early stage of folding controls the formation of the oligomer by domain swapping during protein folding.^[16] The domain-swapped dimer of cyt *c* exhibited different properties from those of its monomer,^[14b, d] although the domain-swapped Mb dimer exhibited a similar oxygen binding character as that of its monomer.^[15] In this study, we show that domain swapping could be used to design a heterodimeric protein of Mb, and this method may be a new approach for creating artificial proteins.

Mb has been favored as a scaffold protein for heme protein design, and has been converted successfully into various artificial enzymes by redesigning its heme active site.^[1b, g, i, m, 2a, b, d, e, 3a-c, 3e, 5e] Although Mb functions in the monomeric form, dimeric Mb was detected more than forty years ago.^[17] We have resolved the X-ray crystallographic structure of dimeric horse Mb (PDB code: 3VM9), which exhibited a unique domain-swapped structure with each active site constructed by two protomers (Figure S1 in the Supporting Information).^[15] Therefore, we chose horse Mb as a model protein, and explored a new approach for designing an artificial protein based on domain swapping.

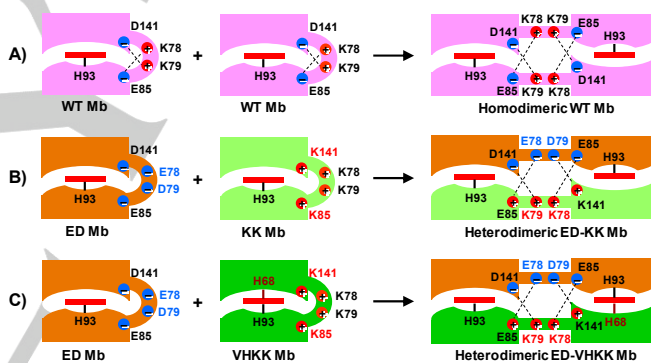


Figure 1. Schematic view of the design of heterodimeric Mb. A) Dimerization of WT Mb; B) Amino acid mutations to control the interaction between the protomers and obtain heterodimeric Mb; C) Amino acid mutations to obtain heterodimeric Mb with two different active sites.

The key initial step for protein design based on dimeric wild-type (WT) horse Mb was to precisely control the dimerization. By close inspection of the X-ray crystallographic structure of dimeric Mb, we found that aside from hydrophobic interactions, four new salt bridges were formed between protomers in the dimer; between Lys78 in one protomer and Glu85 in the other protomer (Lys78_A/Glu85_B), Glu85_A/Lys78_B, Lys79_A/Asp141_B, and Asp141_A/Lys79_B (Figure 1A and Figure S1). Since these residues play an important role in stabilizing the dimer, we envisaged that dimerization of two different mutant Mbs may be controlled by altering these interactions. We replaced the two positively charged residues Lys78 and Lys79 with negatively charged residues (Glu78 and Asp79) in one mutant (K78E/K79D Mb, ED Mb), and the two negatively charged residues Glu85 and Asp141 with positively charged residues (Lys85 and Lys141) in the other mutant (E85K/D141K Mb, KK Mb) (see Figure S2 for locations of the residues in monomeric Mb). We envisaged that the stability of homodimeric Mb of each mutant would decrease by removal of the salt bridges between the protomers due to the mutations (E78/E85 and D79/D141 or K78/K85 and K79/K141), whereas heterodimeric Mb created by ED Mb and KK Mb would be stabilized

[*] Prof. Y.-W. Lin, Dr. S. Nagao, M. Zhang, Prof. S. Hirota
Graduate School of Materials Science, Nara Institute of Science and
Technology, 8916-5 Takayama, Ikoma, Nara, 630-0192, Japan
E-mail: hirota@ms.naist.jp
Prof. Y.-W. Lin
School of Chemistry and Chemical Engineering, University of South
China, Hengyang 421001, China
Dr. Y. Shomura, Prof. Y. Higuchi
Department of Life Science, Graduate School of Life Science,
University of Hyogo, 3-2-1 Koto, Kamigori-cho, Ako-gun, Hyogo 678-
1297, Japan
Dr. Y. Shomura, Prof. Y. Higuchi
RIKEN SPring-8 Center, 1-1-1 Koto, Sayo-cho, Sayo-gun, Hyogo 679-
5148, Japan

[**] We thank Mr. Leigh McDowell for his advice during manuscript
preparation. This work was partially supported by Grants-in-Aid for
Scientific Research from Japan Society for the Promotion of Science
(Category B, No.26288080 (S.H.) and Young Scientists B,
No.24750163 (S.N.)). This work was also supported partially to Y.-W.
L. by the Natural Science Foundation of China (No. 31370812).

Supporting information for this article is available on the WWW under
http://dx.doi.org/10.1002/anie.2014xxxxx.

by the electrostatic interactions between the charge-reversed mutated residues (E78/K85 and D79/K141) (Figure 1B).

ED Mb and KK Mb were purified using a similar procedure reported previously for WT Mb.^[18] We prepared dimeric Mb using the modified procedure for preparation of dimeric WT Mb,^[15] where 10% (v/v) 2-propanol was added to the monomeric Mb solution instead of 5% (v/v) ethanol to obtain a larger amount of dimers (Experimental section in the Supporting Information). Only a small amount (~8%) of homodimers was observed by dimerization of ED Mb with 2-propanol, according to size-exclusion chromatography (Figure 2, curve a, and Figure S3A). The homodimeric ED Mb dissociated completely after heating at 45 °C for 30 min (Figure 2, curve b and Figure S3A). For KK Mb, only the monomer peak was detected in the chromatogram after treatment with 2-propanol, showing that KK Mb did not form homodimers (Figure 2, curve c). When dimers were prepared from a mixture of ED Mb and KK Mb (1:1 ratio) under the same conditions, the amount of dimers obtained increased (~18%) (Figure 2, curve d, and Figure S3B). The dimers obtained from the mixture of ED Mb and KK Mb may contain both homodimeric ED Mb, and the heterodimer of ED Mb and KK Mb (heterodimeric ED-KK Mb). However, after heating the obtained dimer solution (mixture of homodimeric ED Mb and heterodimeric ED-KK Mb) at 45 °C for 30 min, a certain amount of dimer (~12%) was still observable (Figure 2, curve e and Figure S3B). The dimer observed after heating should correspond to heterodimeric ED-KK Mb, since homodimeric ED Mb dissociated by the heating treatment. These results indicate that pure heterodimeric proteins were obtained by controlling the surface charges in domain swapping.

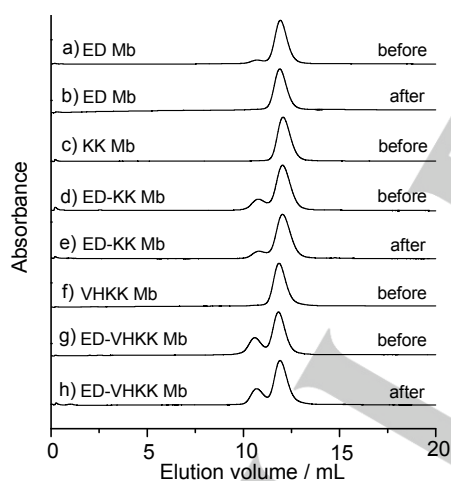


Figure 2. Elution curves of dimeric (a,b) ED Mb, (c) KK Mb, (d,e) ED-KK Mb, (f) VHKK Mb, and (g,h) ED-VHKK Mb treated with 10% (v/v) 2-propanol. The elution curves were taken before (a,c,d,f,g) and after (b,e,h) heating the protein solution at 45 °C for 30 min. Measurement conditions: Column, Superdex 75 10/300 GL; buffer, 50 mM potassium phosphate buffer, pH 7.0; monitoring wavelength, 409 nm; temperature, 4 °C.

We further designed a heterodimeric Mb with two distinct heme coordination sites, which can be found in multi-heme proteins in nature but are hard to achieve in a homodimeric protein.^[19] According to the X-ray crystallographic structure of homodimeric WT Mb (PDB code: 3VM9), the two identical His/H₂O-coordinated heme sites in the dimer are very similar to that in the monomer.^[15] We were interested in whether a bis-His-coordinated heme site, as observed for native neuroglobin^[20] and cytoglobin,^[21] could be generated in one of the two

heme centers in the heterodimer. It has been reported that by exchanging two distal residues, His64 and Val68, with Val and His, respectively (H64V/V68H Mb; Figure S2), His68 and His93 coordinate to the heme iron in both ferric and ferrous states.^[22] Therefore, we referred to the H64V/V68H double mutation to generate a bis-His coordination site at one of the heme sites in heterodimeric Mb, and designed a heterodimer with ED Mb and H64V/V68H/E85K/D141K Mb (VHKK Mb) (Figure 1C). Purified VHKK Mb exhibited similar UV-vis spectra (ferric, peak at 412 nm; ferrous, peaks at 427, 529, and 563 nm; Figure S4C) as those of H64V/V68H Mb,^[22] suggesting that the heme coordination did not alter at either redox state by reversing the charges of two residues at the protein surface. Interestingly, the spectrum of VHKK Mb in the ferrous state resembled those of Mb crystals after X-ray irradiation (529 and 568 nm).^[23]

Heterodimeric ED-VHKK Mb was prepared using the same procedure as that for heterodimeric ED-KK Mb. Similar to KK Mb, VHKK Mb did not form a homodimer by treatment with 2-propanol (Figure 2, curve f), which indicated that the four Lys residues at the protomer interface destabilized the homodimer dramatically, although the bis-His coordination tends to stabilize the dimer. Interestingly, a large amount of dimer (~30%) was observed when constructing dimers from ED Mb and VHKK Mb (Figure 2, curve g, and Figure S3C), and ~24% of dimers were maintained after heating at 45 °C for 30 min (Figure 2, curve h and Figure S3C). The yield of heterodimeric ED-VHKK Mb obtained was more than twice that of heterodimeric ED-KK Mb obtained by the same method, suggesting that the bis-His coordination stabilizes the dimer. After heating the dimer solution at 45 °C for 30 min, we purified heterodimeric ED-VHKK Mb using a Hi-Load Superdex 75 26/60 column, where it was separated from ED Mb and VHKK Mb (Figure S5).

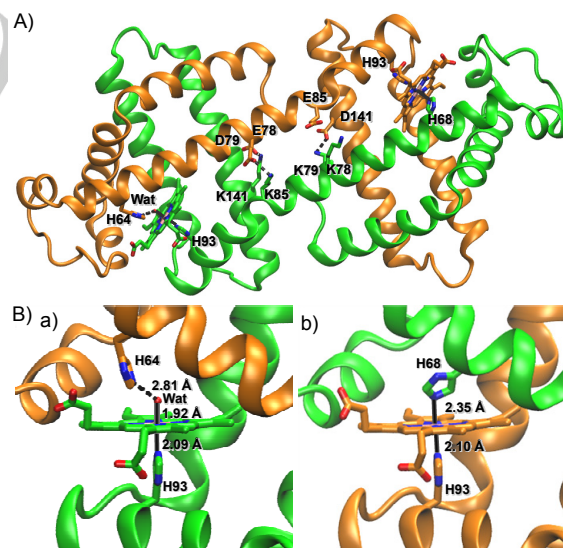


Figure 3. Crystal structure of heterodimeric ED-VHKK Mb (PDB code: 3WYO). A) Overall structure; B) Heme coordination structures: a) His/H₂O and b) bis-His coordination. The coordination bonds and salt bridges are shown in solid and dashed lines, respectively. The hemes and His64, His68, and His93 are shown as stick models. The nitrogen and oxygen atoms of the hemes, His64, His68, His93, the key amino acids of the salt bridges, and coordinated water are shown in blue and red, respectively.

In order to elucidate the structure of heterodimeric ED-VHKK Mb, we performed X-ray crystallographic analysis (PDB code: 3WYO).

The structure at 2.0 Å resolution showed that heterodimeric ED-VHKK Mb adopts a domain-swapped structure identical to that of homodimeric WT Mb (Figure 3A). Three strong salt bridges (E78/K85, 3.20 Å; D79/K141, 2.77 Å; D141/K79, 2.82 Å) were formed in the ED-VHKK Mb heterodimer between the ED Mb and VHKK Mb protomers. However, one salt bridge formed in the WT dimer was not detected in the crystal structure of the heterodimer (E85/K78, 4.83 Å), although it may form weakly in solution by their close arrangements. It was also revealed from the crystal structure that heterodimeric ED-VHKK Mb possesses two heme active sites with different coordination structures, that is, His/H₂O coordination (Figure 3Ba) and bis-His coordination (Figure 3Bb). Distal His64 formed a hydrogen bond (2.81 Å) with the axial water molecule at the His/H₂O-coordinated heme site, similar to that of monomeric Mb.^[18] At the bis-His-coordinated heme site, His68 and His93 coordinated to the heme iron (Fe–His distances: His68, 2.35 Å; His93, 2.10 Å), similar to those in H64V/V68H Mb (His68, 2.31 Å; His93, 2.27 Å).^[22] These observations demonstrate that two distinct heme sites can be designed in a single heterodimeric protein by domain swapping, without large structural alterations from the original site of the monomer.

We investigated the UV-vis spectra of heterodimeric ED-VHKK Mb in different oxidation states, and compared them with those of the original monomers. At the ferric state, the absorption spectrum of ED-VHKK Mb exhibited a Soret band at 410 nm (Figure 4A, black), which was between those of ED Mb (408 nm) and VHKK Mb (412 nm) (Figures S4A and S4C). The spectrum of the visible bands of heterodimeric ED-VHKK overlapped well with the average spectrum of those of ED Mb and VHKK Mb monomers (Figure S6A). By reduction of both heme sites in ED-VHKK Mb with dithionite, the Soret band red-shifted to 427 nm with two visible bands observed at 530 and 563 nm in the spectrum (Figure 4A, red). The spectrum after reduction also overlapped well with the average spectrum of those of ED Mb and VHKK Mb monomers reduced with dithionite (Figure S6B). By reduction with a mild reducing reagent, ascorbic acid, the Soret band of ED-VHKK Mb shifted to 413 nm with a shoulder peak at ~435 nm (Figure 4B). The UV-vis spectrum of heterodimeric ED-VHKK Mb in the presence of ascorbic acid was also similar to the average spectrum of those of ED Mb and VHKK Mb in the presence of ascorbic acid (Figure S6C). ED Mb was reduced to the ferrous deoxy form with ascorbic acid (Figure S4B), whereas VHKK Mb remained in the ferric state (Figure S4D). These results highlight that ED-VHKK Mb contains two distinct heme coordination sites resembling those in ED Mb and VHKK Mb monomers.

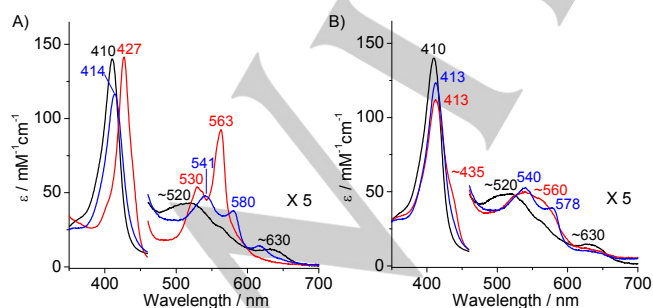
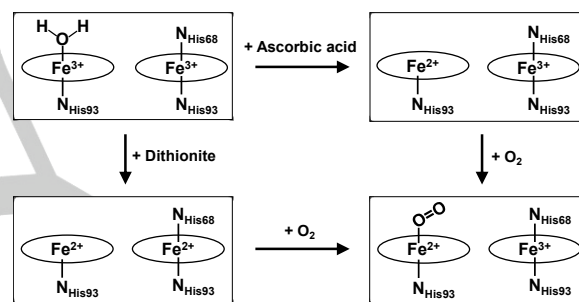


Figure 4. UV-vis spectra of heterodimeric ED-VHKK Mb by reduction with A) dithionite (1 mM) and B) ascorbate (1 mM) in 50 mM potassium phosphate buffer, pH 7.0: Before (black) and after reduction (red), followed by exposure to air (blue).

Scheme 1 illustrates the conversion of the oxidation and coordination states in heterodimeric ED-VHKK Mb by reduction with dithionite or ascorbic acid, and subsequent exposure to air. O₂ bound to the ferrous deoxy heme and an oxygenated complex was formed when fully-reduced (by dithionite) ED-VHKK Mb was exposed to air, as indicated by generation of two visible bands at 541 and 580 nm (Figure 4A, blue). The spectrum obtained following reduction with dithionite and subsequent exposure to air was similar to that of half-reduced (by ascorbic acid) ED-VHKK Mb exposed to air (Figure 4B, blue). The final state obtained after exposure to air contained both a ferric bis-His-coordinated heme and a ferrous oxy heme, since it exhibited a spectrum similar to the average spectra of ferric VHKK Mb and the oxy form of ED Mb (Figure S6D). These results show that the ferrous bis-His heme center in ED-VHKK Mb was quickly oxidized to the ferric state with O₂, similar to the VHKK Mb monomer (Figure S4C), in agreement with the observation for H64V/V68H Mb reported previously.^[22] Therefore, the two hemes may act as two independent sites.

Scheme 1. Conversion of oxidation and coordination states in heterodimeric ED-VHKK Mb with two distinct heme centers.



In conclusion, we demonstrated that protein dimerization by domain swapping can be controlled efficiently through alteration of the salt bridges between the surfaces of two protomers in the dimer. This approach was successfully applied to design a heterodimeric protein of horse Mb with two different heme active sites, which exhibited different ligand binding properties. This study presents a new example for rational protein design with multi-heme groups using domain swapping.

Received: xxxx xx, 20xx

Published online: xxxx xx, 20xx.

Keywords: Crystal structure • Domain swapping • Heme protein • Heterodimer • Protein design

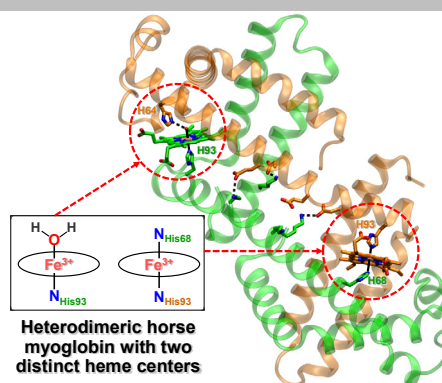
- [1] a) B. Kuhlman, G. Dantas, G. C. Ireton, G. Varani, B. L. Stoddard, D. Baker, *Science* **2003**, *302*, 1364–1368; b) Y. Lu, N. Yeung, N. Sieracki, N. M. Marshall, *Nature* **2009**, *460*, 855–862; c) V. Nanda, R. L. Koder, *Nat. Chem.* **2010**, *2*, 15–24; d) J. Du, M. Sono, J. H. Dawson, *Coord. Chem. Rev.* **2011**, *255*, 700–716; e) M. T. Reetz, *Chem. Rec.* **2012**, *12*, 391–406; f) Y.-T. Lai, D. Cascio, T. O. Yeates, *Science* **2012**, *336*, 1129; g) T. Ueno, H. Tabe, Y. Tanaka, *Chem. Asian J.* **2013**, *8*, 1646–1660; h) Y.-T. Lai, K.-L. Tsai, M. R. Sawaya, F. J. Asturias, T. O. Yeates, *J. Am. Chem. Soc.* **2013**, *135*, 7738–7743; i) Y.-W. Lin, E. B. Sawyer, J. Wang, *Chem. Asian J.* **2013**, *8*, 2534–2544; j) M. L. Zastrow, V. L. Pecoraro, *Coord. Chem. Rev.* **2013**, *257*, 2565–2588; k) H. C. Fry, A. Lehmann, L. E. Sinks, I. Asselberghs, A. Tronin, V. Krishnan, J. K. Blasie, K. Clays, W. F. DeGrado, J. G. Saven, M. J. Therien, *J. Am. Chem. Soc.* **2013**, *135*, 13914–13926; l) T. A.

- Farid, G. Kodali, L. A. Solomon, B. R. Lichtenstein, M. M. Sheehan, B. A. Fry, C. Bialas, N. M. Ennist, J. A. Siedlecki, Z. Zhao, M. A. Stetz, K. G. Valentine, J. L. Anderson, A. J. Wand, B. M. Discher, C. C. Moser, P. L. Dutton, *Nat. Chem. Biol.* **2013**, *9*, 826–833; m) Y.-W. Lin, J. Wang, Y. Lu, *Sci. China Chem.* **2014**, *57*, 346–355; n) Y. Li, P. C. Cirino, *Biotechnol. Bioeng.* **2014**, *111*, 1273–1287; o) B. Höcker, *Curr. Opin. Struct. Biol.* **2014**, *27C*, 56–62; p) M. Dürrenberger, T. R. Ward, *Curr. Opin. Chem. Biol.* **2014**, *19*, 99–106; q) O. Shoji, Y. Watanabe, *J. Biol. Inorg. Chem.* **2014**, *19*, 529–539.
- [2] a) K. D. Miner, A. Mukherjee, Y.-G. Gao, E. L. Null, I. D. Petrik, X. Zhao, N. Yeung, H. Robinson, Y. Lu, *Angew. Chem. Int. Ed.* **2012**, *51*, 5589–5592; b) X. Liu, Y. Yu, C. Hu, W. Zhang, Y. Lu, J. Wang, *Angew. Chem. Int. Ed.* **2012**, *51*, 4312–4316; c) A. J. Reig, M. M. Pires, R. A. Snyder, Y. Wu, H. Jo, D. W. Kulp, S. E. Butch, J. R. Calhoun, T. G. Szyperski, E. I. Solomon, W. F. DeGrado, *Nat. Chem.* **2012**, *4*, 900–906; d) K. Oohora, Y. Kihira, E. Mizohata, T. Inoue, T. Hayashi, *J. Am. Chem. Soc.* **2013**, *135*, 17282–17285; e) Y.-B. Cai, X. H. Li, J. Jing, J. L. Zhang, *Metallics* **2013**, *5*, 828–835.
- [3] a) N. Yeung, Y.-W. Lin, Y.-G. Gao, X. Zhao, B. S. Russell, L. Lei, K. D. Miner, H. Robinson, Y. Lu, *Nature* **2009**, *462*, 1079–1082; b) Y.-W. Lin, N. Yeung, Y.-G. Gao, K. D. Miner, S. Tian, H. Robinson, Y. Lu, *Proc. Natl. Acad. Sci. USA* **2010**, *107*, 8581–8586; c) Y.-W. Lin, N. Yeung, Y.-G. Gao, K. D. Miner, L. Lei, H. Robinson, Y. Lu, *J. Am. Chem. Soc.* **2010**, *132*, 9970–9972; d) M. Tegoni, F. Yu, M. Bersellini, J. E. Penner-Hahn, V. L. Pecoraro, *Proc. Natl. Acad. Sci. USA* **2012**, *109*, 21234–21239; e) Q. Zhou, M. Hu, W. Zhang, L. Jiang, S. Perrett, J. Zhou, J. Wang, *Angew. Chem. Int. Ed.* **2013**, *52*, 1203–1207.
- [4] a) S. D. Khare, Y. Kipnis, P. Greisen, Jr., R. Takeuchi, Y. Ashani, M. Goldsmith, Y. Song, J. L. Gallaher, I. Silman, H. Leader, J. L. Sussman, B. L. Stoddard, D. S. Tawfik, D. Baker, *Nat. Chem. Biol.* **2012**, *8*, 294–300; b) M. L. Zastrow, A. F. Peacock, J. A. Stuckey, V. L. Pecoraro, *Nat. Chem.* **2012**, *4*, 118–123; c) B. S. Der, D. R. Edwards, B. Kuhlman, *Biochemistry* **2012**, *51*, 3933–3940; d) V. M. Cangelosi, A. Deb, J. E. Penner-Hahn, V. L. Pecoraro, *Angew. Chem. Int. Ed.* **2014**, *53*, 7900–7903.
- [5] a) R. J. Radford, J. D. Brodin, E. N. Salgado, F. A. Tezcan, *Coord. Chem. Rev.* **2011**, *255*, 790–803; b) A. F. A. Peacock, *Curr. Opin. Chem. Biol.* **2013**, *17*, 934–939; c) C. J. Reedy, B. R. Gibney, *Chem. Rev.* **2004**, *104*, 617–649; d) A. Roy, I. Sarrou, M. D. Vaughn, A. V. Astashkin, G. Ghirlanda, *Biochemistry* **2013**, *52*, 7586–7594; e) K. Oohora, T. Hayashi, *Curr. Opin. Chem. Biol.* **2014**, *19*, 154–161.
- [6] M. Russwurm, D. Koesling, *Mol. Cell. Biochem.* **2002**, *230*, 159–164.
- [7] J. Bos, F. Fusetti, A. J. Driessen, G. Roelfes, *Angew. Chem. Int. Ed.* **2012**, *51*, 7472–7475.
- [8] a) M. J. Bennett, M. P. Schlunegger, D. Eisenberg, *Protein Sci.* **1995**, *4*, 2455–2468; b) Y. Liu, D. Eisenberg, *Protein Sci.* **2002**, *11*, 1285–1299; c) M. E. Newcomer, *Curr. Opin. Struct. Biol.* **2002**, *12*, 48–53; d) F. Rousseau, J. W. Schymkowitz, L. S. Itzhaki, *Structure* **2003**, *11*, 243–251; e) M. J. Bennett, M. R. Sawaya, D. Eisenberg, *Structure* **2006**, *14*, 811–824; f) A. M. Gronenborn, *Curr. Opin. Struct. Biol.* **2009**, *19*, 39–49.
- [9] K. J. Knaus, M. Morillas, W. Swietnicki, M. Malone, W. K. Surewicz, V. C. Yee, *Nat. Struct. Biol.* **2001**, *8*, 770–774.
- [10] R. Janowski, M. Kozak, E. Jankowska, Z. Grzonka, A. Grubb, M. Abrahamson, M. Jaskolski, *Nat. Struct. Biol.* **2001**, *8*, 316–320.
- [11] C. Liu, M. R. Sawaya, D. Eisenberg, *Nat. Struct. Mol. Biol.* **2011**, *18*, 49–55.
- [12] M. Yamasaki, T. J. Sendall, M. C. Pearce, J. C. Whisstock, J. A. Huntington, *EMBO Rep.* **2011**, *12*, 1011–1017.
- [13] a) D. Nurizzo, M. C. Silvestrini, M. Mathieu, F. Cutruzzola, D. Bourgeois, V. Fülöp, J. Hajdu, M. Brunori, M. Tegoni, C. Cambillau, *Structure* **1997**, *5*, 1157–1171; b) B. R. Crane, R. J. Rosenfeld, A. S. Arvai, D. K. Ghosh, S. Ghosh, J. A. Tainer, D. J. Stuehr, E. D. Getzoff, *EMBO J.* **1999**, *18*, 6271–6281; c) M. Czjzek, S. Létoffé, C. Wandersman, M. Delepierre, A. Lecroisey, N. Izadi-Pruneyre, *J. Mol. Biol.* **2007**, *365*, 1176–1186; d) M. A. Silva, T. G. Lucas, C. A. Salgueiro, C. M. Gomes, *PLoS One* **2012**, *7*, e46328.
- [14] a) S. Hirota, Y. Hattori, S. Nagao, M. Taketa, H. Komori, H. Kamikubo, Z. Wang, I. Takahashi, S. Negi, Y. Sugiura, M. Kataoka, Y. Higuchi, *Proc. Natl. Acad. Sci. USA* **2010**, *107*, 12854–12859; b) Z. Wang, T. Matsuo, S. Nagao, S. Hirota, *Org. Biomol. Chem.* **2011**, *9*, 4766–4769; c) Y. Hayashi, S. Nagao, H. Osuka, H. Komori, Y. Higuchi, S. Hirota, *Biochemistry* **2012**, *51*, 8608–8616; d) S. Junedi, K. Yasuhara, S. Nagao, J. Kikuchi, S. Hirota, *ChemBioChem* **2014**, *15*, 517–521.
- [15] S. Nagao, H. Osuka, T. Yamada, T. Uni, Y. Shomura, K. Imai, Y. Higuchi, S. Hirota, *Dalton Trans.* **2012**, *41*, 11378–11385.
- [16] a) P. P. Parui, M. S. Deshpande, S. Nagao, H. Kamikubo, H. Komori, Y. Higuchi, M. Kataoka, S. Hirota, *Biochemistry* **2013**, *52*, 8732–8744; b) M. S. Deshpande, P. P. Parui, H. Kamikubo, M. Yamanaka, S. Nagao, H. Komori, M. Kataoka, Y. Higuchi, S. Hirota, *Biochemistry* **2014**, *53*, 4696–4703.
- [17] A. H. van den Oord, J. J. Westdorp, A. F. van Dam, J. A. Verheij, *Eur. J. Biochem.* **1969**, *10*, 140–145.
- [18] R. Maurus, C. M. Overall, R. Bogumil, Y. Luo, A. G. Mauk, M. Smith, G. D. Brayer, *Biochim. Biophys. Acta* **1997**, *1341*, 1–13.
- [19] K. D. Bewley, K. E. Ellis, M. A. Firer-Sherwood, S. J. Elliott, *Biochim. Biophys. Acta* **2013**, *1827*, 938–948.
- [20] A. Pesce, S. Dewilde, M. Nardini, L. Moens, P. Ascenzi, T. Hankeln, T. Burmester, M. Bolognesi, *Structure* **2003**, *11*, 1087–1095.
- [21] D. de Sanctis, S. Dewilde, A. Pesce, L. Moens, P. Ascenzi, T. Hankeln, T. Burmester, M. Bolognesi, *J. Mol. Biol.* **2004**, *336*, 917–927.
- [22] Y. Dou, S. J. Admiraal, M. Ikeda-Saito, S. Krzywdka, A. J. Wilkinson, T. Li, J. S. Olson, R. C. Prince, I. J. Pickering, G. N. George, *J. Biol. Chem.* **1995**, *270*, 15993–16001.
- [23] H.-P. Hersleth, K. K. Andersson, *Biochim. Biophys. Acta* **2011**, *1814*, 785–796.

Artificial Multi-heme Protein

COMMUNICATION

Protein design is a useful method to create novel artificial proteins. We rationally designed an artificial heterodimeric protein with two different heme active sites (a bis-histidine-coordinated heme and a H₂O/histidine-coordinated heme) using domain swapping for horse myoglobin (see figure). The developed method is useful for designing artificial multi-heme proteins.



*Ying-Wu Lin, Satoshi Nagao, Mohan Zhang, Yasuhito Shomura, Yoshiki Higuchi, and Shun Hirota**

Page No. – Page No.

Rational Design of Heterodimeric Protein Using Domain Swapping for Myoglobin

Contents

1. Experimental section	p. S2
Preparation of Mb mutants	
Preparation and analysis of dimeric Mb	
X-ray crystallography	
UV-vis measurements	
2. Table S1. Statistics of data collection and structure refinement of heterodimeric ED-VHKK Mb.	p. S5
3. Figure S1. X-ray crystallographic structure of dimeric wild-type horse Mb.	p. S6
4. Figure S2. Locations of mutated residues in monomeric Mb.	p. S7
5. Figure S3. Elution curves of dimeric ED Mb, ED-KK Mb, and ED-VHKK Mb.	p. S8
7. Figure S4. UV-vis spectra of monomeric ED Mb and VHKK Mb reduced with dithionite or ascorbic acid.	p. S9
6. Figure S5. Elution curves of dimeric ED-VHKK Mb.	p. S10
8. Figure S6. Comparison of UV-vis spectra of heterodimeric ED-VHKK Mb with an average of those of monomeric ED Mb and VHKK Mb.	p. S11

Experimental section

Preparation of Mb mutants

Mb mutants genes were constructed using the KOD Plus Mutagenesis Kit (Toyoba, Japan), and confirmed by DNA sequencing (ABI PRISM 310 genetic analyzer sequencing system, Applied Biosystems, Inc.). E85K/D141K Mb (KK Mb), H64V/V68H/E85K/D141K Mb (VHKK Mb), and K78E/K79D Mb (ED Mb) were expressed in *Escherichia coli* LE392 cells. All mutants were purified using a procedure described previously.¹ The primers used for generating the mutations are as follows:

K78E primers:

P-fwd: 5'-GAA AAA GGG CAC CAC GAA GCT GAG CTC A-3'

P-rev: 5'-CTT AAG GAT GCC ACC TAG GGC AGT TAA-3'

K79D primers based K78E mutation:

P-fwd: 5'-GAT GGG CAC CAC GAA GCT GAG CTC AAA CCG-3'

P-rev: 5'-TTC CTT AAG GAT GCC ACC TAG GGC AGT-3'

E85K primers:

P-fwd: 5'-AAG CTC AAA CCG CTT GCG CAA TCG CAT G-3'

P-rev: 5'-AGC TTC GTG GTC CCC TTT TTT CTT AAG-3'

D141K primers:

P-fwd: 5'-AAG ATC GCT GCT AAG TAC AAA GAA CTG GGT-3'

P-rev: 5'-GTT ACG GAA CAG CTC GAG AGC TTT GGT-3'

V68H primers:

P-fwd: 5'-CAT TTA ACT GCC CTA GGT GGC ATC CTT AAG-3'

P-rev: 5'-AAC GGT GCC ATG TTT TTT CAG ATC TTC-3'

H64V primers based on V68H mutation:

P-fwd: 5'-GTT GGC ACC GTT CAT TTA ACT GCC CTA GG-3'

P-rev: 5'-TTT TTT CAG ATC TTC AGA CGC CTT CAT-3'

Preparation and analysis of dimeric Mb

Dimeric Mbs were prepared by dissolving 0.3 mM ED Mb, KK Mb, VHKK Mb, ED Mb/KK Mb mixture (1:1), or ED Mb/VHKK Mb mixture in 50 mM potassium phosphate buffer, pH 7.0, followed by addition of 10% (v/v) 2-propanol on ice for 15 min and subsequent lyophilization. The obtained precipitate was dissolved again in 50 mM potassium phosphate buffer, pH 7.0. After filtration, the produced dimeric Mb

was purified by gel chromatography (HiLoad 26/60 Superdex 75, GE healthcare) using a fast protein liquid chromatography (FPLC) system (BioLogic DuoFlow 10, Bio-Rad, CA).² In the preparation of ED-KK Mb and ED-VHKK Mb heterodimers, the obtained solution containing dimeric Mb was heated at 45 °C for 30 min before loading on the HiLoad gel column. For elucidating the stability of the dimer, the ratio of the monomer and dimer after incubation at 45 °C for 15 or 30 min was analyzed with a Superdex 75 10/300 gel column under the same conditions.

X-ray crystallography

Crystallization was carried out at 277 K using the sitting drop vapor diffusion method with crystal plates (CrystalClear D Strips, Douglas Instruments, Hampton Research, CA). The protein concentration was adjusted to 3.6 mM in 50 mM potassium phosphate buffer, pH 7.0. The droplet prepared by mixing 2 μ L of the protein solution with 2 μ L of the reservoir solution was equilibrated. The reservoir solution consisted of 25% (w/v) PEG 1000 and 100 mM MES-NaOH buffer, pH 6.5. The diffraction data were collected at the BL38B1 beam line at SPring-8, Japan. The crystal was mounted on a cryo-loop and flash-frozen at 100 K in a nitrogen cryo system. An ADSC Q315 detector was used. The diffraction data were processed using the program HKL2000.³ The preliminary structure was obtained by the molecular replacement method (MOLREP),⁴ using the atomic coordinates of the structure of horse Mb (PDB code: 1WLA) as a starting model. Structural refinement was performed using the program REFMAC.⁵ The molecular model was manually corrected, and water molecules were picked up in the electron density map using the program COOT.⁶ The data collection and refinement statistics are summarized in Table S1.

UV-vis measurements

Absorption spectra were measured with a UV-2450 spectrophotometer (Shimadzu, Japan) using a 1-cm path-length quartz cell at 25°C. Proteins were dissolved in 50 mM potassium phosphate buffer, pH 7.0. Protein concentrations were determined using the pyridine method as reported,⁷ where the absorption coefficient for the Soret band at 408, 412, and 410 nm were determined to be 173, 144, and 140 $\text{mM}^{-1}\text{cm}^{-1}$ for ED Mb, VHKK Mb, and ED-VHKK Mb heterodimers, respectively.

References

1. S. Hirota, K. Azuma, M. Fukuba, S. Kuroiwa, N. Funasaki. *Biochemistry*, **2005**, *44*, 10322–10327.
2. S. Nagao, H. Osuka, T. Yamada, T. Uni, Y. Shomura, K. Imai, Y. Higuchi, S. Hirota, *Dalton Trans.*, **2012**, *41*, 11378–11385.
3. Z. Otwinowski, W. Minor, *Methods Enzymol.* **1997**, *276*, 307–326.
4. A. Vagin, A. Teplyakov, *J. Appl. Cryst.* **1997**, *30*, 1022–1025.
5. G. N. Murshudov, P. Skubák, A. A. Lebedev, N. S. Pannu, R. A. Steiner, R. A. Nicholls, M. D. Winn, F. Long, A. A. Vagin, *Acta Crystallogr. Sect. D* **2011**, *67*, 355–367.
6. P. Emsley, K. Cowtan, *Acta Crystallogr. Sect. D* **2004**, *60*, 2126–2132.
7. E. A. Berry, B. L. Trumpower. *Anal. Biochem.* **1987**, *161*, 1–15.

Table S1. Statistics of data collection and structure refinement of heterodimeric ED-VHKK Mb (PDB code: 3WYO).

Data collection	
X-ray source	SPring-8 (BL38B1)
Wavelength (Å)	1.0000
Space group	<i>P</i> 2 ₁ 2 ₁ 2 ₁
Unit cell parameters <i>a</i> , <i>b</i> , <i>c</i> (Å)	55.7, 72.2, 161.5
Resolution (Å)	20.00–2.00 (2.05–2.00)
Number of unique reflections	45097 (2198)
<i>R</i> _{merge} ^a	0.073 (0.630)
Completeness (%)	100.0 (100.0)
$\langle I/\sigma(I) \rangle$	27.0 (2.9)
Redundancy	7.5 (6.1)
Refinement	
Resolution (Å)	20.00–2.00 (2.05–2.00)
Number of reflections	39225 (1680)
<i>R</i> _{work} ^b	0.228 (0.262)
<i>R</i> _{free} ^b	0.266 (0.318)
Completeness (%)	91.3 (51.5)
Number of atoms in an asymmetric unit	
Protein	4824
Water	355
Heme	172
Average <i>B</i> factors (Å ²)	
Protein	33.8
Water	30.4
Heme	24.5
Ramachandran plot (%)	
Favored	96.5
Allowed	3.5
Outlier	0.0

Statistics for the highest-resolution shell are given in parentheses.

$$^a R_{\text{merge}} = \frac{\sum_{\text{hkl}} |I - \langle I \rangle|}{(\sum_{\text{hkl}} I)^{-1}}$$

^b $R_{\text{work}} = \frac{\sum_{\text{hkl}} ||F_{\text{obs}}| - k|F_{\text{calc}}||}{(\sum_{\text{hkl}} |F_{\text{obs}}|)^{-1}}$, *k*: scaling factor. *R*_{free} was computed identically, except where all reflections belong to a test set of 5 % of randomly selected data.

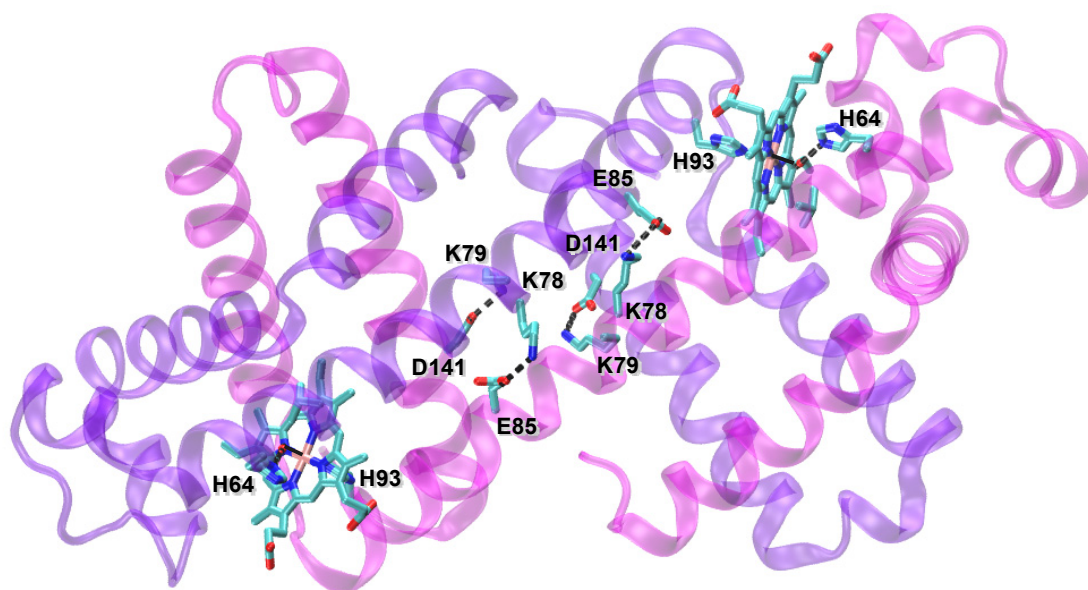


Figure S1. X-ray crystallographic structure of dimeric wild-type horse Mb (PDB code: 3VM9). Two heme active sites and four salt bridges (two pairs of salt bridges; Lys78/Glu85, Lys79/Asp141, Glu85/Lys78, and Asp141/Lys79) between the protomers are shown. The coordination bonds and salt bridges are shown in solid and dashed lines, respectively. The nitrogen and oxygen atoms of the hemes, His64, His93, the key amino acids of the salt bridges, and coordinated water are shown in blue and red, respectively.

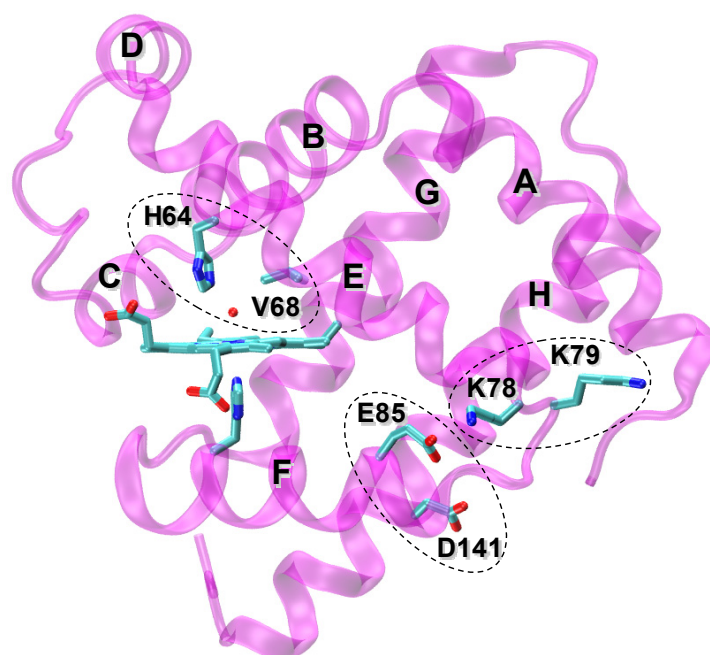


Figure S2. Locations of mutated residues in monomeric Mb (PDB code: 1WLA) for the design of heterodimeric Mb. Helices A–H are labeled. Mutated residues are shown as stick models and indicated in dashed circles. The heme is also shown as a stick model. The nitrogen and oxygen atoms of the hemes, mutated amino acids, and coordinated water are shown in blue and red, respectively.

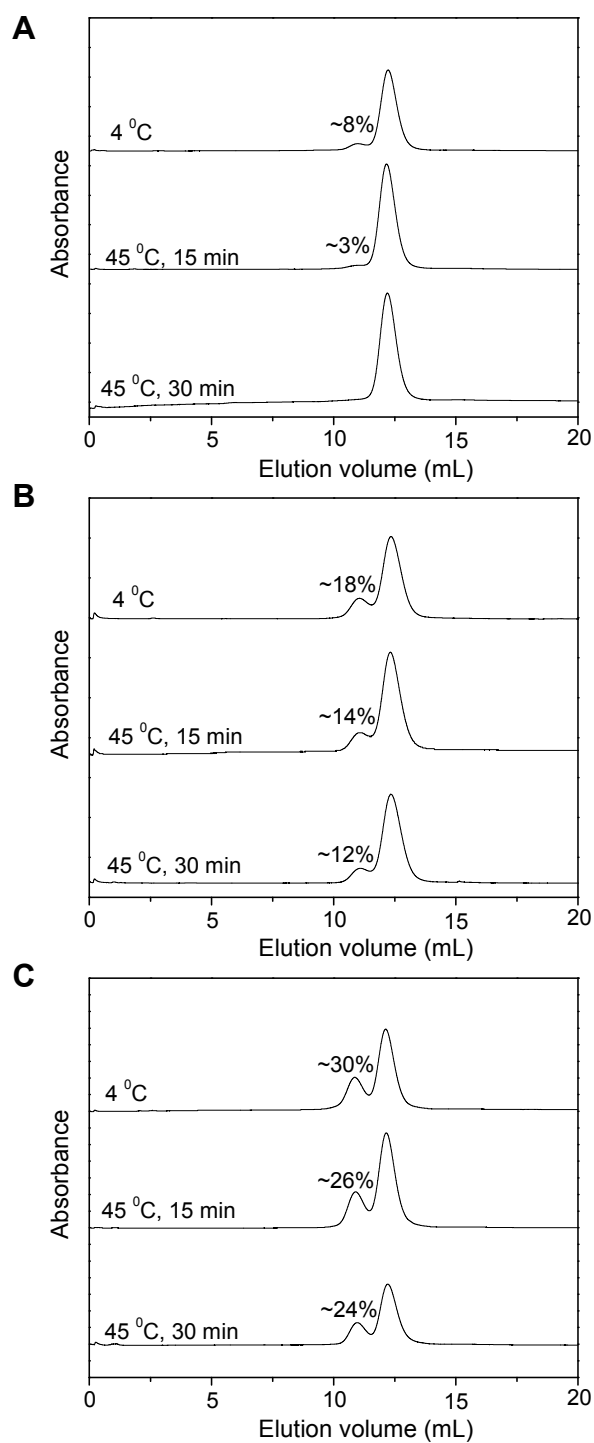


Figure S3. Elution curves of dimeric (A) ED Mb, (B) ED-KK Mb, and (C) ED-VHKK Mb treated with 2-propanol. Elution curves were taken before and after heating the protein solution at 45 °C for 15 and 30 min. Measurement conditions: Column, Superdex 75 10/300 GL; buffer, 50 mM potassium phosphate buffer, pH 7.0; monitoring wavelength, 409 nm; temperature, 4 °C.

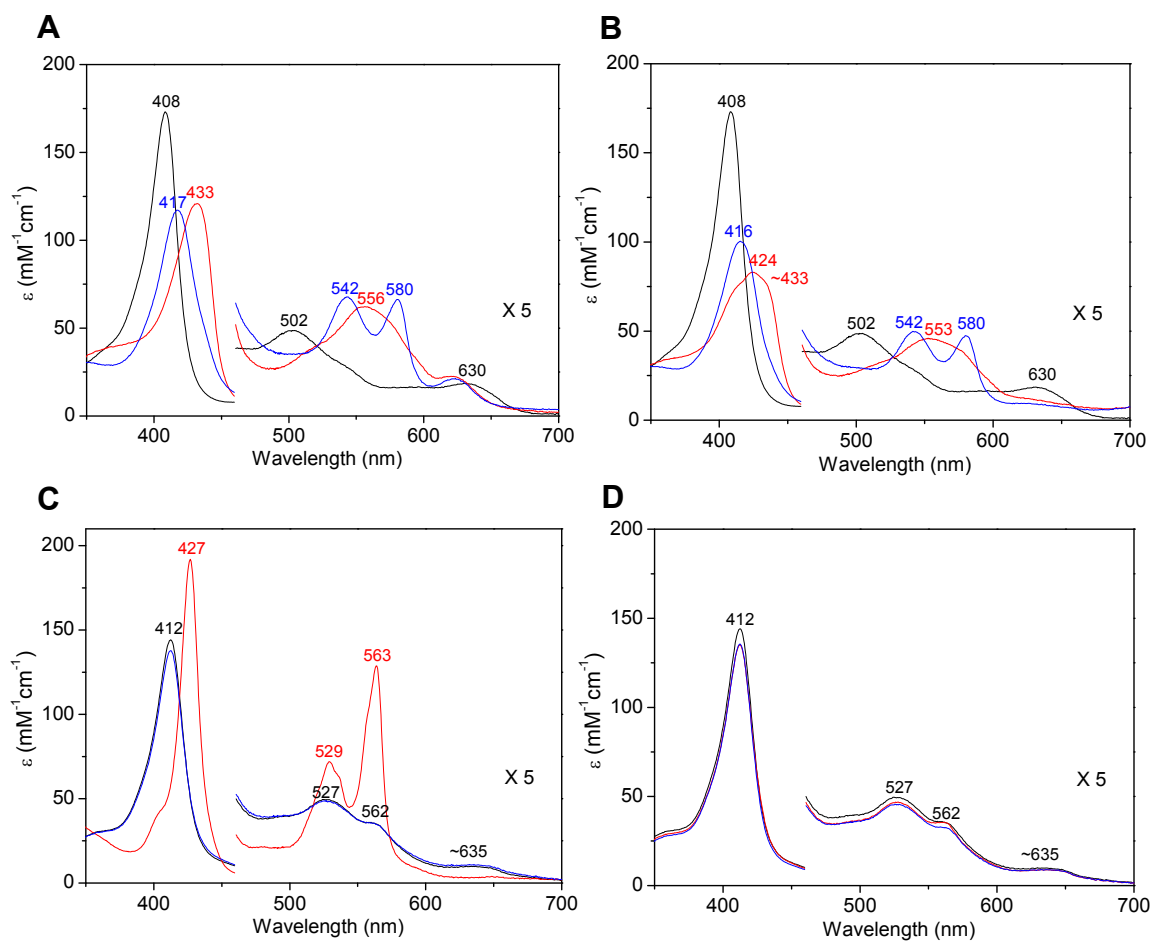


Figure S4. UV-vis spectra of monomeric (A, B) ED Mb and (C, D) VHKK Mb reduced with (A, C) dithionite (1 mM) and (B, D) ascorbic acid (1 mM) in 50 mM potassium phosphate buffer, pH 7.0. The spectra were taken before (black) and after (red) an addition of dithionite or ascorbic acid, and subsequent exposure to air (blue).

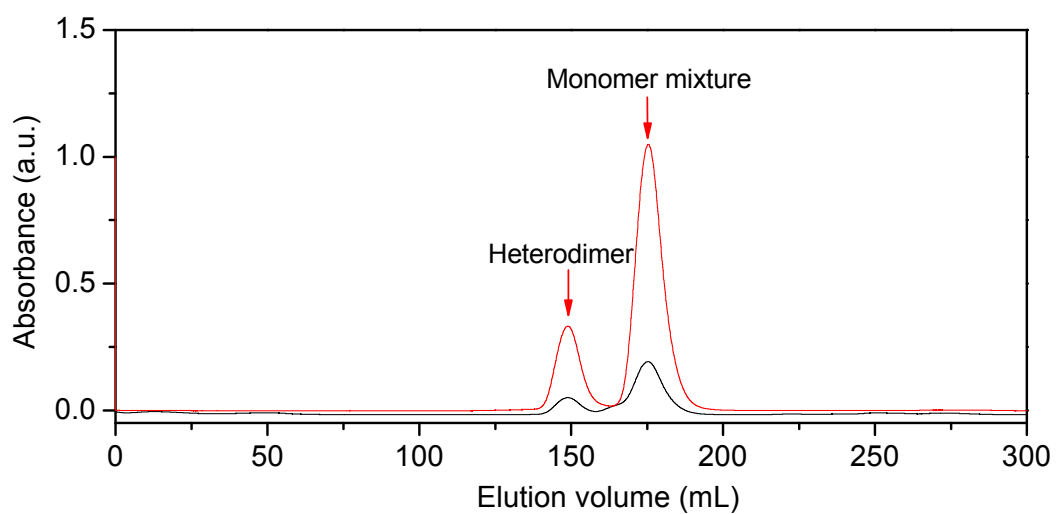


Figure S5. Elution curves of dimeric ED-VHKK Mb after treatment with 2-propanol and heating at 45 °C for 30 min. Measurement conditions: Column, Hi-Load Superdex 75 26/60; buffer, 50 mM potassium phosphate buffer, pH 7.0; monitoring wavelength, 280 nm (black) and 409 nm (red); temperature, 4 °C.

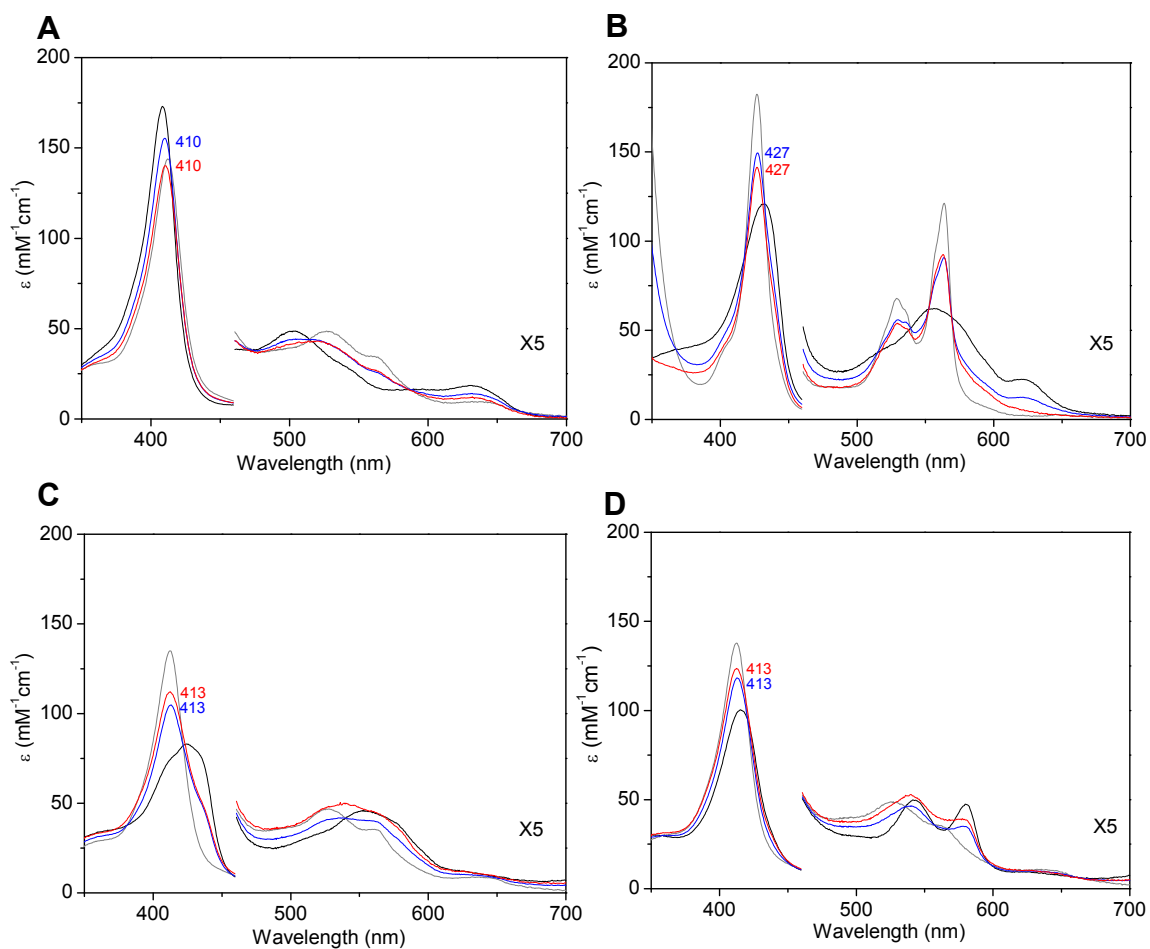


Figure S6. Comparison of UV-vis spectra of heterodimeric ED-VHKK Mb with an average spectra of those of monomeric ED Mb and VHKK Mb: (A) ferric form, (B) fully reduced form obtained by an addition of 1 mM dithionite, (C) half-reduced form obtained by an addition of 1 mM ascorbic acid, and (D) the spectra obtained by exposure to air after reduction with 1 mM dithionite. Black, ED Mb; gray, VHKK Mb; blue, average spectrum of ED Mb and VHKK Mb; red, heterodimeric ED-VHKK Mb.